Materials Chemistry

Cite this: *J. Mater. Chem.*, 2011, **21**, 6995

www.rsc.org/materials

PAPER

In situ immobilization of Ag nanoparticles on Keggin heteropoly blue microtubes†

Yan Shen,[a] Jun Peng,*[a] Huanqiu Zhang,[a] Changyun Chen,[a] Fang Zhang[a] and Alan M. Bond*[b]

Received 8th January 2011, Accepted 17th March 2011
DOI: 10.1039/c1jm10114e

Silver nanoparticles (NPs)-deposited tungstosilicate ($Ag/SiW_{12}/Ag$) microtubes were obtained by a redox reaction between the heteropoly blue microtubes and Ag^+ ions. The $Ag/SiW_{12}/Ag$ microtubes were characterized by FT-IR and XPS spectroscopy. Their morphology was examined by ESEM-FEG, showing that the microtubes kept their original microtubular morphology well after reacting with Ag^+ ions and the silver NPs exhibited regular spherical morphology. The current–voltage properties of the $Ag/SiW_{12}/Ag$ microtubes were also briefly investigated.

Introduction

Polyoxometalates (POMs) are known as a unique class of inorganic compounds with tunable compositional diversity, structural versatility and redox properties, which have potential applications in the areas of catalysis, medicine as well as functional materials.[1–7] POMs can be reduced to heteropoly blues (HPBs) by undergoing stepwise multi-electron redox processes without any structural change. HPBs are a large class of mixed-valence POMs.[8,9] The strong reduction capability of HPBs has been used in the synthesis of zero valent state metal nanoparticles (NPs).[10] Papaconstantinou and coworkers provided a comprehensive study on photochemical redox interactions between POMs, such as $[SiW_{12}O_{40}]^{4-}$, $[PW_{12}O_{40}]^{3-}$, $[P_2W_{18}O_{62}]^{6-}$ and $[P_2Mo_{18}O_{62}]^{6-}$, and various metal ions like Ag^+, Pd^{2+}, Au^{3+}, Cu^{2+}, Hg^{2+}, *etc.*[11–13] By a suitable choice of POMs and organic substrate, some metal ions can be reduced to a lower or zero oxidation state. The metal NPs prepared in preappointed nano- or micro-meter scale locations by POMs in solid substrates were also achieved. For example, Wu reported the controllable *in situ* synthesis of metal NPs in a POM hybrid film by utilizing electron and proton transfer between surfactant and POM,[14] and the controllable *in situ* incorporation of metal NPs in silica spheres through the photoreduction of POMs well-dispersed in a hydrophobic microenvironment.[15]

Presently, morphology-tunable nano- and micro-scale materials based on POMs have been extensively researched. Some research groups have been focused on nano- and micro-tubes of POMs for exerting both merits of POMs and tubular morphology.[16–18] We have reported the template-free aqueous synthesis of α-$K_4SiW_{12}O_{40}$ microtubes[19] and ascorbic acid-doped Keggin POM microtubes.[20] On the basis of these investigations, we have obtained the HPB microtubes. Noble metal NPs can be immobilized on the surfaces of the HPB microtubes to obtain composite tubular materials containing both hollow cylindrical POMs and metal NPs, which may have potential applications in catalysis and microelectronics, *etc.* Herein we report silver NPs-deposited tungstosilicate ($Ag/SiW_{12}/Ag$) microtubes synthesized by the redox reaction between the HPB microtubes and Ag^+ ions. In addition, current–voltage (*I–V*) measurements indicated that the electrical conductivity of SiW_{12} microtubes undergoes a notable increase after deposition of silver NPs.

Experimental

Chemicals and measurements

Monolacunary tungstosilicate $K_8[\alpha\text{-}SiW_{11}O_{39}]$ (α-SiW_{11}) was synthesized according to the published procedure.[21] Ascorbic acid ($C_6H_8O_6$), HCl, NH_3, $AgNO_3$, C_2H_5OH, $Na_2C_2O_4$, $KMnO_4$ and H_2SO_4 were of analytical grade. All the chemicals were used directly without any further purification. All aqueous solutions were made with deionized water.

FT-IR spectra were recorded on a D/MAX-IIIC instrument. XPS measurements were carried out on a Thermo ESCALAB 250 spectrometer with an Al–Kα (1486.6 eV) achromatic X-ray source. ESEM-FEG images were acquired with an XL30 Field-Emission Environmental Scanning Electron Microscope. The *I–V* (current–voltage) measurements were obtained on a Keithley 4200 SCS instrument.

[a]*Key Laboratory of Polyoxometalate Science of the Ministry of Education, Faculty of Chemistry, Northeast Normal University, Changchun, Jilin, 130024, People's Republic of China. E-mail: jpeng@nenu.edu.cn*
[b]*School of Chemistry, Monash University, Clayton, Victoria, 3800, Australia. E-mail: alan.bond@sci.monash.edu.au*

† Electronic supplementary information (ESI) available: Plot of electron number *vs.* the mole number of AA in HPB-i (i = 1–4); ESEM images and EDS spectra of the outside wall of SiW_{12} and $Ag/SiW_{12}/Ag$ microtubes; XPS spectrum of silver particles in $Ag/SiW_{12}/Ag$ microtubes; ESEM images of Ag NPs and the statistical size distributions derived from the outside and inside wall of $Ag/SiW_{12}/Ag$ microtubes obtained from HPB-i (i = 1–3). See DOI: 10.1039/c1jm10114e

Preparation of Ag/SiW_{12}/Ag microtubes

Ag/SiW_{12}/Ag microtubes were synthesized through three steps: first, preparation of SiW_{12}-AA microtubes; second, preparation of HPB microtubes; last, preparation of Ag/SiW_{12}/Ag microtubes.

SiW_{12}-AA microtubes were synthesized according to the literature method.[20] In a typical preparation process for SiW_{12}-AA microtubes, α-$K_8[SiW_{11}O_{39}]$ (3 g, 1 mmol) were added in deionized water (10 mL) under stirring. Then 3 $molL^{-1}$ HCl was added dropwise until the solid dissolved completely and the pH reached 1. This solution was heated in a 80 °C water bath for 15 min, after which 0.082 g of AA (ascorbic acid, 0.5 mmol) was added. The resulting solution was heated for 5 min. Tubular clusters grew rapidly in seconds on the beaker bottom after cooling to room temperature (25 °C) for about 10 min. They were harvested after careful filtration and dried in air. As the SiW_{12}-AA microtubes were intermediate products of the HPB microtubes, different amounts of AA were used to obtain the HPB microtubes with different degrees of reduction. The batch of as-prepared SiW_{12}-AA microtubes using 0.082 g of AA was labeled "SiW_{12}-AA-1". In turn, the batch of as-prepared SiW_{12}-AA microtubes was labeled "SiW_{12}-AA-2" when using 0.164 g of AA (1 mmol), "SiW_{12}-AA-3" when using 0.246 g of AA (1.5 mmol), "SiW_{12}-AA-4" when using 0.328 g of AA (2 mmol). The results of TG (thermogravimetry) and element analyses indicate that the practically doped amount of AA into the SiW_{12} microtubes is approximately a quarter of the experimentally added amount.

HPB-i (i = 1–4) microtubes were prepared from the corresponding SiW_{12}-AA-i (i = 1–4) microtubes by putting the tubular samples on a piece of filter paper, and exposing to ammonia atmosphere. The tubular samples changed color from brown to dark blue.

Ag/SiW_{12}/Ag microtubes were prepared through a redox reaction between HPB microtubes and $AgNO_3$. In a typical preparation process, the HPB microtubes were put on a piece of glass substrate, then a few drops of $AgNO_3$ saturated ethanol solution were dropped rapidly on to the glass slice to cover the HPB microtubes completely. The HPB microtubes adsorbed the $AgNO_3$ solution through surface adsorption and capillary suction;[22] meanwhile silver nanoparticles were deposited on the POM microtubes to obtain brownish black Ag/SiW_{12}/Ag microtubes after evaporation of ethanol.

Results and discussion

Characterization of the intermediate product HPB microtubes

Our previous work has shown that the SiW_{12}-AA microtubes can change to a blue color in ammonia, and the coloration of the microtubes is due to the speed up of redox reaction between the AA and SiW_{12} as the basicity increases. Herein we use this method to obtain HPB-i (i = 1–4) microtubes from the SiW_{12}-AA-i (i = 1–4) microtubes (Scheme 1).

The morphology of the HPB microtubes was determined by examination of the optical micrograph (Fig. 1) and was the same as that of the precursor SiW_{12}-AA microtubes. The basic length of the HPB microtubes is around 3 mm; the inner diameter is in the range of 40–100 μm; the wall thickness is in the range of 20–50 μm.

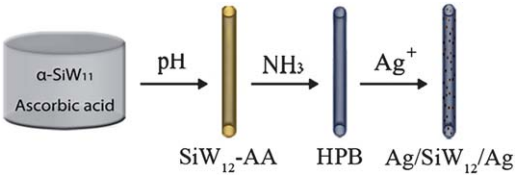

Scheme 1 Process for preparation of the Ag/SiW_{12}/Ag microtubes.

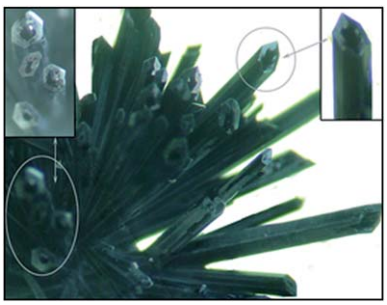

Fig. 1 An optical micrograph of the HPB microtubes.

Potassium permanganate titration was used to determine the degree of reduction of HPB-i (i = 1–4) microtubes (Figure S1†). The plot of electron number of the HPB-i (i = 1–4) microtubes *vs.* the mole number of AA in HPB-i (i = 1–4) microtubes is linear. The redox titration results show that the more AA in SiW_{12}-AA, the higher the extent of reduction for the HPB microtubes, until the degree of reduction approaches 1e per HPB. The reduction level is always less than 2e, as theoretically expected for AA, which is probably accounted for by partial oxidation of the HPB microtubes by oxygen present in the air.

Characterization of Ag/SiW_{12}/Ag microtubes

The characterization of Ag/SiW_{12}/Ag microtubes was performed by taking the sample prepared from HPB-4 microtubes. For a comparison, IR spectra of SiW_{12}, HPB-4 and the Ag/SiW_{12}/Ag microtubes are compared in Fig. 2. The IR spectrum of HPB-4 microtubes shows the characteristic vibration absorption peaks of α-SiW_{12} with slight shifts due to the redistribution of charge density in the oxygen atoms because of the increase of negative

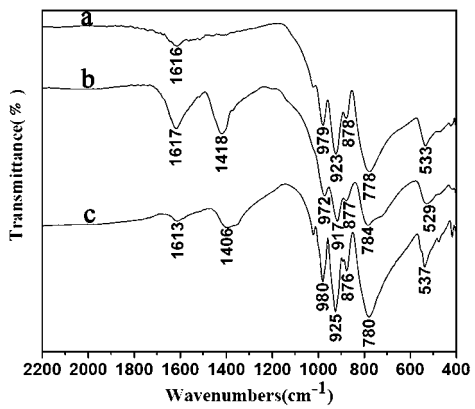

Fig. 2 IR spectra of SiW_{12} (a), HPB-4 (b) and the Ag/SiW_{12}/Ag (c) microtubes.

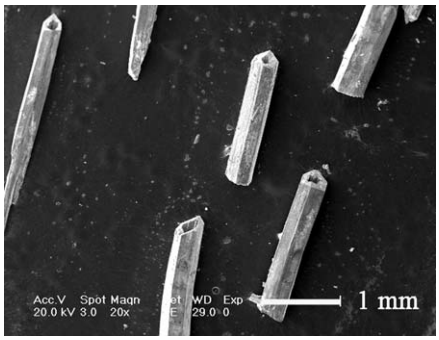

Fig. 3 ESEM image of Ag/SiW_{12}/Ag microtubes.

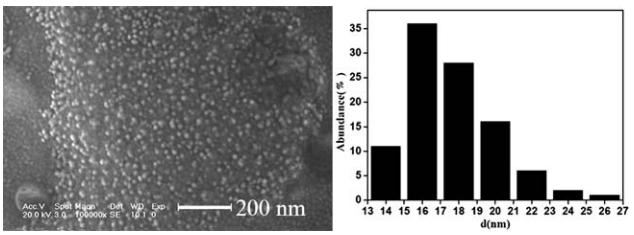

Fig. 4 ESEM image of Ag NPs on the outside wall of Ag/SiW_{12}/Ag microtubes (left) and the statistical size distribution (right), obtained from HPB-4.

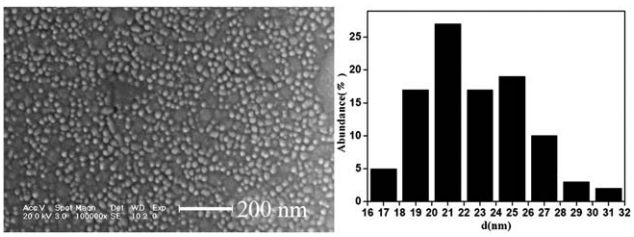

Fig. 5 ESEM image of Ag NPs on the inside wall of Ag/SiW_{12}/Ag microtubes (left) and the statistical size distribution (right), obtained from HPB-4.

charge of the POM anion, while the peak positions in the IR spectrum of Ag/SiW_{12}/Ag microtubes restore to those of α-SiW_{12} with a full oxidation state, which supports that a redox reaction has occurred between HPB and Ag^+ ions. The new vibration absorption peaks at 1418 cm^{-1} and 1406 cm^{-1} are attributable to $\nu_{(N-H)}$ of the incorporated NH_3 molecules, which act as proton acceptors in the SiW_{12}-AA microtubes and exist as NH_4^+ cations in the HPB and Ag/SiW_{12}/Ag microtubes.

The generation of silver NPs can be distinguished easily from the ESEM images of the microtube surfaces with silver and without silver (Figure S2 a, b†), and the corresponding EDS spectra confirm the exist of silver (Figure S2 c, d†). The original microtubular morphology was still kept after immobilization of Ag NPs (Fig. 3). XPS measurements were made to characterize the deposition of Ag NPs (Figure S3†), which demonstrates that the binding energy of Ag $3d_{5/2}$ is 368.2 eV, attributed to elemental silver.

The morphology and distribution of the silver NPs on the two sides of the wall of Ag/SiW_{12}/Ag microtubes, corresponding to parent HPB-4 measured by ESEM are shown in Fig. 4 and 5. The

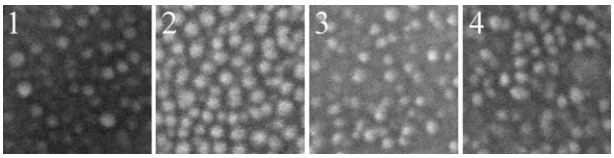

Fig. 6 ESEM images of Ag NPs on the outside wall of Ag/SiW_{12}/Ag microtubes obtained by HPB-i (i = 1–4) microtubes (All these areas are 200 × 200 nm^2).

ESEM images exhibit regular spherical morphology of Ag NPs. The sizes of the Ag NPs on the outside wall of the microtubes are narrowly distributed between 15 and 25 nm, but the sizes of the Ag NPs broaden to 50 nm on the inside wall of the microtubes, perhaps relevant to the rates of redox reaction and conglomeration of Ag NPs, influenced by the degree of reduction of the HPB microtubes, evaporation rate of ethanol and other factors. The ESEM images and size distributions of the silver particles for the other three HPB-i (i = 1–3) are presented in Figures S4–5†.

Effect of the degree of reduction of the SiW_{12} Keggin entity on the formation of Ag NPs

We intended to find how the degree of reduction of SiW_{12} Keggin entity would influence the growth of Ag NPs by using the four HPB-i (i = 1–4) microtubes as reductants. Fig. 6 shows the ESEM images of Ag NPs on the surfaces of Ag/SiW_{12}/Ag microtubes obtained by HPB-i (i = 1–4) microtubes. From these images we find that the morphologies and sizes of Ag NPs are basically the same. This fact indicates that the degree of reduction of HPB microtubes does not significantly affect the growth of Ag NPs. A probable explanation is that the redox reaction is not dependent on the concentration of the reductant HPB microtubes as reaction occurs on the surface. In addition, the rapid evaporation rate of ethanol is another key factor. Generally, in the initial reduction period, metal ions are reduced to form small clusters, and further reduction of metal ions as well as their agglomeration occur during the growth phase.[23,24] Once the solvent ethanol is evaporated, the formation and agglomeration of Ag NPs will stop and the Ag NPs formed will be incorporated on the surface of the microtubes. In summary, probably the factors determining the morphology and size of Ag NPs are the solid HPB microtubes that serve as a reductant and a substrate for Ag NPs and the ethanol that serve as the medium for the formation and agglomeration of Ag NPs.

The *I–V* property of Ag/SiW_{12}/Ag microtubes

I–V measurements were carried out for individual SiW_{12} microtube (Fig. 7) and Ag/SiW_{12}/Ag microtube (Fig. 8) respectively.[25,26] To carry out *I–V* measurements, a microtube was placed on a glass substrate, coated with silver paste on both ends of the microtube to form electrodes. The conductance of individual Ag/SiW_{12}/Ag microtube estimated from the *I–V* curve is approximately six times as much as that of a SiW_{12} microtube, which shows that electrical conductivity of the POM microtubes has notably increased after deposition of silver NPs.

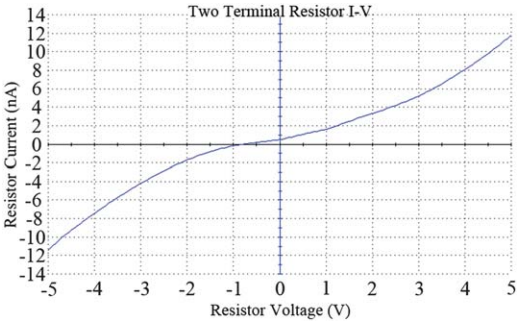

Fig. 7 The *I–V* curve of an individual SiW_{12} microtube.

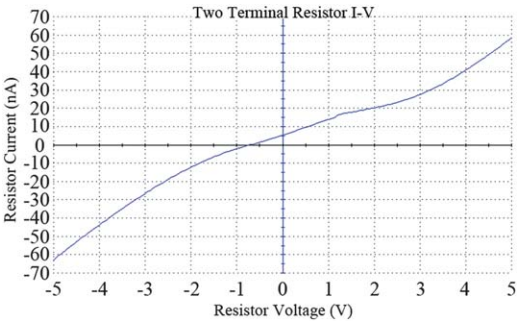

Fig. 8 The *I–V* curve of an individual Ag/SiW_{12}/Ag microtube.

Conclusion

We have presented a convenient and mild method for immobilization of Ag NPs on POM microtubes. This method is relatively non-toxic and inexpensive. The Ag NPs obtained show a spherical morphology and a uniform distribution on the two sides of the wall of the POM microtubes. The noble metal can be recycled by simply dissolving the POM microtubes. The Ag/SiW_{12}/Ag mictotubes exhibit enhanced electrical conductivity. This work shows the significance of design, preparation and application of composite microtubes containing both POM and metal NP components. Moreover, immobilization of NPs on microtubes may provide an opportunity to investigate the interactions of nano and *meso* materials. Qualitative examination of the oxidation of ethanol vapor using Ag/SiW_{12}/Ag microtubes as a catalyst shows the potential for Ag/SiW_{12}/Ag microtubes in the catalysis field. Future work will explore catalytic applications in more detail.

Acknowledgements

This work was financially supported by the National Natural Science Foundation of China (Grant 21071029) and the Australian Research Council.

Notes and references

1 A. Haimov, H. Cohen and R. Neumann, *J. Am. Chem. Soc.*, 2004, **126**, 11762.
2 D. A. Judd, J. H. Nettles, N. Nevins, J. P. Snyder, D. C. Liotta, J. Tang, J. Ermolieff, R. F. Schinazi and C. L. Hill, *J. Am. Chem. Soc.*, 2001, **123**, 886.
3 Q. S. Yin, J. M. Tan, C. Besson, Y. V. Geletii, D. G. Musaev, A. E. Kuznetsov, Z. Luo, K. I. Hardcastle and C. L. Hill, *Science*, 2010, **328**, 342.
4 B. Keita, T. B. Liu and L. Nadjo, *J. Mater. Chem.*, 2009, **19**, 19.
5 Z. H. Kang, C. H. A. Tsang, Z. D. Zhang, M. L. Zhang, N. B. Wong, J. A. Zapien, Y. Y. Shan and S. T. Lee, *J. Am. Chem. Soc.*, 2007, **129**, 5326.
6 Z. H. Kang, C. H. A. Tsang, N. B. Wong, Z. D. Zhang and S. T. Lee, *J. Am. Chem. Soc.*, 2007, **129**, 12090.
7 Z. H. Kang, E. B. Wang, B. D. Mao, Z. M. Su, L. Gao, S. Y. Lian and L. Xu, *J. Am. Chem. Soc.*, 2005, **127**, 6534.
8 M. I. Khan, Q. Chen and J. Zubieta, *Inorg. Chem.*, 1993, **32**, 2924.
9 N. Casañ-Pastor, P. Gomez-Romero, G. B. Jameson and L. C. W. Baker, *J. Am. Chem. Soc.*, 1991, **113**, 5658.
10 S. Mandal, P. R. Selvakannan, R. Pasricha and M. Sastry, *J. Am. Chem. Soc.*, 2003, **125**, 8440.
11 A. Troupis, A. Hiskia and E. Papaconstantinou, *Angew. Chem., Int. Ed.*, 2002, **41**, 1911.
12 A. Troupis, A. Hiskia and E. Papaconstantinou, *Appl. Catal., B*, 2003, **42**, 305.
13 A. Hiskia, E. Papaconstantinou and A. Troupis-Koukoutsis, *PCT Int. Appl.*, 2006, PIXXD2 WO 2006038045 A1 20060413.
14 W. Qi, H. L. Li and L. X. Wu, *J. Phys. Chem. B*, 2008, **112**, 8257.
15 Y. Y. Zhao, W. Qi, W. Li and L. X. Wu, *Langmuir*, 2010, **26**, 4437.
16 Z. H. Kang, E. B. Wang, M. Jiang, S. Y. Lian, Y. G. Li and C. W. Hu, *Eur. J. Inorg. Chem.*, 2003, 370.
17 R. Y. Wang, D. Z. Jia, L. Zhang, L. Liu, Z. P. Guo, B. Q. Li and J. X. Wang, *Adv. Funct. Mater.*, 2006, **16**, 687.
18 J. Li, X. H. Wang, W. M. Zhu and F. H. Cao, *ChemSusChem*, 2009, **2**, 177.
19 Z. F. Xin, J. Peng, T. Wang, B. Xue, Y. M. Kong, L. Li and E. B. Wang, *Inorg. Chem.*, 2006, **45**, 8856.
20 Y. Shen, J. Peng, H. J. Pang, P. P. Zhang, D. Chen, C. Y. Chen, H. Q. Zhang, C. L. Meng and Z. M. Su, *Chem.–Eur. J.*, 2011, **17**, 3657.
21 A. Tézé and G. Hervé, *J. Inorg. Nucl. Chem.*, 1977, **39**, 999.
22 B. M. Kim, S. Z. Qian and H. H. Bau, *Nano Lett.*, 2005, **5**, 873.
23 P. K. Sudeep and P. V. Kamat, *Chem. Mater.*, 2005, **17**, 5404.
24 M. Kavitha, M. R. Parida, E. Prasad, C. Vijayan and P. C. Deshmukh, *Macromol. Chem. Phys.*, 2009, **210**, 1310.
25 L. Liu, H. X. Li, D. Y. Tu, Z. Y. Ji, C. S. Wang, Q. X. Tang, M. Liu, W. P. Hu, Y. Q. Liu and D. B. Zhu, *J. Am. Chem. Soc.*, 2006, **128**, 12917.
26 Q. X. Guo, H. B. Tang, Y. J. Liu, Y. L. Zhang, W. P. Li, S. Hu and D. B. WangZhu, *J. Am. Chem. Soc.*, 2008, **130**, 9198.

